

## 2*p*-insulator heterointerfaces: Creation of half-metallicity and anionogenic ferromagnetism via double exchange

Baomin Zhang,<sup>1,\*</sup> Chonglong Cao,<sup>1</sup> Guowei Li,<sup>2</sup> Feng Li,<sup>1</sup> Weixiao Ji,<sup>1</sup> Shufeng Zhang,<sup>1</sup> Miaojuan Ren,<sup>1</sup> Haikun Zhang,<sup>1</sup> Rui-Qin Zhang,<sup>3</sup> Zhicheng Zhong,<sup>4</sup> Zhe Yuan,<sup>5</sup> Shengjun Yuan,<sup>6,†</sup> and Graeme R. Blake<sup>2,‡</sup>

<sup>1</sup>*School of Physics and Technology, University of Jinan, 250022 Jinan, P. R. China*

<sup>2</sup>*Zernike Institute for Advanced Materials, University of Groningen, 9747 AG Groningen, The Netherlands*

<sup>3</sup>*Department of Physics and Materials Science, City University of Hong Kong, Hong Kong SAR, P. R. China*

<sup>4</sup>*Ningbo Institute of Materials Technology and Engineering (NIMTE), Chinese Academy of Sciences, 315201 Ningbo, P. R. China*

<sup>5</sup>*The Center for Advanced Quantum Studies and Department of Physics, Beijing Normal University, 100875 Beijing, P. R. China*

<sup>6</sup>*School of Physics and Technology, Wuhan University, 430072 Wuhan, P. R. China*



(Received 28 September 2017; revised manuscript received 25 January 2018; published 6 April 2018)

We use first-principles calculations to predict the occurrence of half-metallicity and anionogenic ferromagnetism at the heterointerface between two 2*p* insulators, taking the KO<sub>2</sub>/BaO<sub>2</sub> (001) interface as an example. Whereas a sharp heterointerface is semiconducting, a heterointerface with a moderate concentration of swapped K and Ba atoms is half-metallic and ferromagnetic at ambient pressure due to the double exchange mechanism. The K-Ba swap renders the interfacial K-O and Ba-O atomic layers electron-doped and hole-doped, respectively. Our findings pave the way to realize metallicity and ferromagnetism at the interface between two 2*p* insulators, and such systems can constitute a new family of heterostructures with novel properties, expanding studies on heterointerfaces from 3*d* insulators to 2*p* insulators.

DOI: [10.1103/PhysRevB.97.165109](https://doi.org/10.1103/PhysRevB.97.165109)

### I. INTRODUCTION

Materials containing magnetic 3*d* or 4*f* ions have been widely studied and are generally well understood. Recently, research into magnetic materials has begun to extend to systems where magnetism originates from 2*p* orbitals [1]. Due to the more delocalized character of *p* orbitals and their tendency toward electron pairing when forming covalent bonds, magnetic materials based on 2*p* orbitals are relatively rare. Solid molecular oxygen (O<sub>2</sub>) is a paradigm for magnetism arising from 2*p* orbitals, and the spins order antiferromagnetically below a Néel temperature of 24 K [2]. Three charged dioxygen species exist: the dioxygenyl cation (O<sub>2</sub><sup>+</sup>), the superoxide anion (O<sub>2</sub><sup>-</sup>), and the peroxide anion (O<sub>2</sub><sup>2-</sup>). Dioxygenyl salts are Mott insulators [3], metal superoxides are correlated materials serving as suitable model systems for studying intrinsic 2*p* magnetism, and metal peroxides are nonmagnetic due to the pairing of electrons in the antibonding  $\pi^*$  orbital [4]. In the past decade, much progress on this class of insulating materials has been achieved, including studies on correlation effect [5–8], 2*p* orbital ordering [9–12], low-dimensional magnetism [13–15], short-range ferromagnetism [16], frustrated magnetism [6,17–19], interplay of spin, charge, orbital and lattice degrees of freedom [12,20–24], and half-metallicity at high pressure [25]. However, the realization of metallicity and long-range ferromagnetism at ambient

pressure are still lacking, and they remain central topics in this field.

It is useful to draw an analogy with the well-known double exchange mechanism [26,27] that is commonly observed in the alkaline earth (AE) metal-doped manganite perovskite series La<sub>1-x</sub>AE<sub>x</sub>MnO<sub>3</sub> [28], which contains mixed-valent Mn<sup>3+</sup> and Mn<sup>4+</sup>. As is shown in Fig. 1, the Mn<sup>4+</sup> cation has empty  $e_g$  orbitals, whereas those of the Mn<sup>3+</sup> cation are singly occupied. Consequently, the simultaneous hopping (with special spin selection due to strong Hund's coupling) of conducting electrons from Mn<sup>3+</sup> to Mn<sup>4+</sup> renders these materials ferromagnetic and metallic. Very similarly, the O<sub>2</sub><sup>2-</sup> anion has fully occupied  $\pi^*$  orbitals whereas the O<sub>2</sub><sup>-</sup> anion has one unpaired electron. Consequently, we might expect that the simultaneous hopping (with special spin selection due to Pauli exclusion principle) of conducting electrons from O<sub>2</sub><sup>2-</sup> to O<sub>2</sub><sup>-</sup> can also render the exchange between anions ferromagnetic in the mixed-valent alkali (A) metal sesquioxides A<sub>2</sub>O<sub>3</sub>. However, experimental studies of these compounds have thus far found only spin-glass states with insulating characters [5,17–19].

Here, we propose an alternative way to induce double exchange in 2*p* insulators: the fabrication of heterointerfaces between an alkali superoxide AO<sub>2</sub> and an alkaline earth peroxide AEO<sub>2</sub>, by analogy with the widely studied heterointerfaces between two insulators with similar structures (such as LaAlO<sub>3</sub>/SrTiO<sub>3</sub>) grown by the pulsed laser deposition (PLD) or molecular beam epitaxy (MBE) method. Many intriguing phenomena have been reported for the last of these, including a two-dimensional electron gas (2DEG) [29], charge ordering (CO) and orbital ordering (OO) [30], superconductivity [31], magnetism [32], and even the coexistence of the above [33–35]). Similarly, due to the structural similarities, the

\*sps\_zhangbm@ujn.edu.cn

†s.yuan@whu.edu.cn

‡g.r.blake@rug.nl

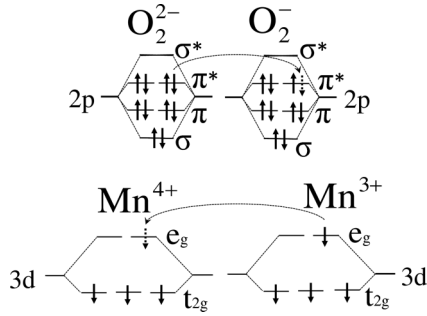


FIG. 1. Double exchange can occur between peroxide ( $\text{O}_2^{2-}$ ) and superoxide ( $\text{O}_2^-$ ) anions, analogous to the situation involving  $\text{Mn}^{3+}$  and  $\text{Mn}^{4+}$  cations.

fabrication of  $\text{AO}_2/\text{AEO}_2$  heterointerfaces by the PLD or MBE method is possible, and fancy electronic and magnetic properties are also expected.

A well-studied example is the  $\text{CaRuO}_3/\text{CaMnO}_3$  (001) interface where the interfacial ferromagnetism and metallicity are induced via double exchange between  $\text{Mn}^{3+}$  and  $\text{Mn}^{4+}$  cations at the interface [36–38]. In a similar fashion, we show in this study that double exchange between  $\text{O}_2^{2-}$  and  $\text{O}_2^-$  anions at an  $\text{AO}_2/\text{AEO}_2$  interface can serve as a reliable mechanism to induce emergent half-metallicity and ferromagnetism. We use density functional theory (DFT) calculations to study the electronic and magnetic properties of  $\text{KO}_2/\text{BaO}_2$  heterostructures along the [001] direction, where mixed-valent dioxygen anions coexist such that double exchange is likely. We find that sharp interfaces are semiconducting because double exchange is weak, whereas rough interfaces at which  $\text{K}^+$  and  $\text{Ba}^{2+}$  are swapped are half-metallic and ferromagnetic due to stronger double exchange.

## II. COMPUTATIONAL DETAILS

All the DFT calculations were carried out from first principles using the PBE generalized gradient approximation (GGA) as the exchange correlation functional [39]. The projector augmented-wave method was employed [40,41], as implemented in the Vienna Ab Initio Simulation Package (VASP) [42–45]. Considering the correlation effect in superoxides and peroxides, a value of Hubbard  $U = 4$  eV was used for the  $2p$  orbitals of oxygen for all calculations (unless otherwise specified) within the framework of  $\text{GGA} + U$  [46], which is the same as the value of Hubbard  $U$  used in previous studies on  $\text{KO}_2$  [9] and  $\text{CsO}_2$  [13]. The core levels, which were kept frozen during calculations, consisted of orbitals up to and including the  $2p$  levels for K,  $4d$  level for Ba, and  $1s$  level for O. The energy cutoff for the plane wave basis set was 400 eV. Optimization of the internal atomic positions were performed (while the cell shape and volume are kept fixed) on every supercell described below, and the convergence criteria for force and energy were  $0.02$  eV/Å and  $0.01$  meV, respectively. The crystal structure of  $\text{BaO}_2$  were fully optimized, including the shape and volume of the conventional unit cell, and the positional parameters as well; the optimized lattice parameters in the  $a - b$  plane agreed well with the experimental values within a discrepancy of 0.8%, and they were chosen as the

in-plane lattice parameters of the basic unit of the supercell. For all supercells used in this paper, the thickness of the vacuum region in the slab model was chosen to be  $13$  Å to reduce the mirror image effect to a negligible value. To calculate the accurate density of states (DOS), supercells with sizes of  $2a \times 2a$  and  $4a \times 4a$  ( $a$  is the optimized lattice parameter of  $\text{BaO}_2$  in the  $a - b$  plane) in the  $a - b$  plane were used, and their Brillouin-zone integrations used a  $\Gamma$ -centered  $k$ -mesh  $12 \times 12 \times 1$  and  $6 \times 6 \times 1$ , respectively.

When studying the electronic and magnetic properties of heterostructures with sharp and rough interfaces, we used the slab model. For the case with a sharp interface, the slab (whose size in the  $a - b$  plane is  $2a \times 2a$ ) contained 6 K-O and 7 Ba-O atomic layers (156 atoms in total), as shown in Fig. 2(a). For the case with a rough interface (swapped K-Ba), the supercell is based on that with the sharp interface, with the main difference that one K in the interfacial K-O layer is swapped with one Ba in the interfacial Ba-O layer, as shown in Fig. 2(b).

The heterostructure before relaxation is constructed as follows: For the  $\text{KO}_2$  side, we adopt the same tilting pattern of oxygen dimers and distortion of cation lattice as what was reported on  $\text{KO}_2$  [9]. For the  $\text{BaO}_2$  side, its basic unit is the same as that in the fully optimized tetragonal cell. Moreover, the distance between the first K-O layer and first Ba-O layer is chosen as the average between the distance of two adjacent K-O layers and that of two adjacent Ba-O layers. When the optimization is finished, we find the following. For the case where the interface is sharp, neither distortion of cation lattice nor tilting of oxygen dimers is found in the  $\text{BaO}_2$  side. In the  $\text{KO}_2$  side, no tilting of oxygen dimers is found, but we find a very similar distortion of cation lattice compared to what was reported on  $\text{KO}_2$  by Nandy *et al.* [9]. The square lattice of K distorts into a pattern of rhombus, and this zigzag distortion of  $\text{K}^+$  cations leads to a degeneracy lifting of the degenerate  $\pi^*$  levels, similar to what happened in the well-known Jahn-Teller effect in transition metal oxides. The only difference is that the magnitude of the distortion here is about  $0.11$  Å, smaller than what was reported previously, and this is probably due to the compressive strain in K-O layers suffered from the Ba-O layers. For the case where the interface is rough, neither distortion of cation lattices nor tilting of oxygen dimers is found in the  $\text{BaO}_2$  side. In the  $\text{KO}_2$  side, no tilting of oxygen dimers is found. For the distortion of cation lattice, from the second K-O layer to the sixth K-O layer, the magnitude of the distortion is also about  $0.11$  Å, while there is no distortion of cation lattice in the first K-O layer, which is due to the metallicity of this layer originating from double exchange.

To study the influence of the concentration of these  $\text{K}_{\text{Ba}}/\text{Ba}_{\text{K}}$  defect complexes on the occurrence of half-metallicity and ferromagnetism at the rough interface, we studied four cases with defect concentrations of 6.25% (case *a*), 12.5% (case *b*), 25% (case *c*), and 50% (case *d*) K-Ba in the interfacial layers. That is, the percentage indicate the proportion of K (Ba) atoms in the first K-O (first Ba-O) layer that were swapped. Calculations were performed using four supercells: In case *a*, the size of the supercell in the  $a - b$  plane is  $4a \times 4a$ , and it consists of 480 atoms (5 K-O and 5 Ba-O atomic layers). This supercell contains only one K-Ba swap (the defect concentration is  $1/16$ ) at the interface, and the

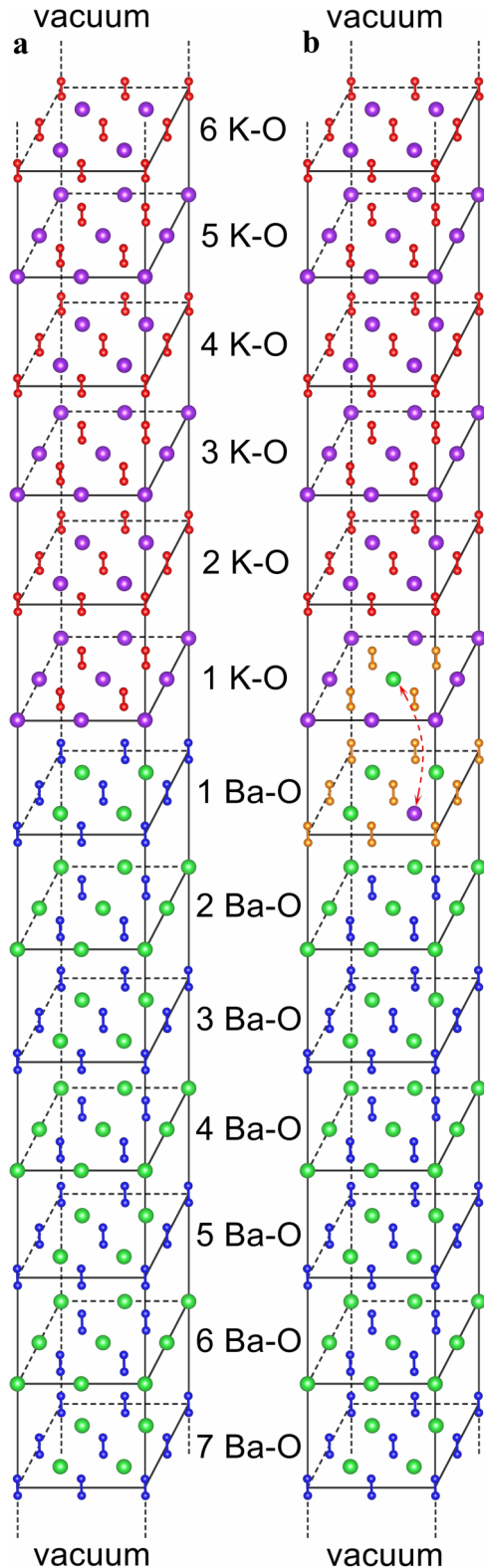


FIG. 2. Supercells used to model heterostructures with (a) a sharp interface, (b) a rough interface (swapped K-Ba). The purple and green spheres represent K and Ba atoms, respectively. The red and blue dimers represent O<sub>2</sub><sup>2-</sup> and O<sub>2</sub><sup>-</sup>, respectively. The yellow dimers indicate dioxxygen anions with stronger mixed valence character in the case with a rough interface. Please note that the small distortion of K<sup>+</sup> cation lattice is not shown in these two cases for the clarity of the picture.

shortest distance between neighboring defects is  $4a$ . In case *b*, the size of the supercell in the  $a - b$  plane is also  $4a \times 4a$ , and it again consists of 480 atoms (5 K-O and 5 Ba-O atomic layers). The supercell contains two K-Ba swaps (the defect concentration is  $1/8$ ) at the interface, and the shortest distance between neighboring defects is  $2\sqrt{2}a$ . In case *c*, the size of the supercell in the  $a - b$  plane is  $2a \times 2a$ , and it consists of 120 atoms (5 K-O and 5 Ba-O atomic layers). It contains only one K-Ba swap (the defect concentration is  $1/4$ ) at the interface, and the shortest distance between neighboring defects is  $2a$ . In case *d*, the size of the supercell in the  $a - b$  plane is  $2a \times 2a$ , and it again consists of 120 atoms (5 K-O and 5 Ba-O atomic layers). It contains two K-Ba swaps (the defect concentration is  $1/2$ ) at the interface, and the shortest distance between neighboring defects is  $\sqrt{2}a$ .

### III. RESULTS AND DISCUSSIONS

We choose the KO<sub>2</sub>/BaO<sub>2</sub> (001) heterostructure as our example, where the (001) surfaces of these two constituent compounds are both nonpolar surfaces. And the two compounds both adopt the body-centered tetragonal CaC<sub>2</sub> structure type with space group  $I4/mmm$  at room temperature [47,48]. In KO<sub>2</sub> (BaO<sub>2</sub>), each oxygen dimer O<sub>2</sub><sup>-</sup> (O<sub>2</sub><sup>2-</sup>) is 6-fold coordinated by K<sup>+</sup> (Ba<sup>2+</sup>) cations forming a quasi-octahedron which is slightly elongated along  $c$  axis. The KO<sub>2</sub>/BaO<sub>2</sub> (001) interface is expected to be stable for two main reasons. First, the experimental lattice parameters of KO<sub>2</sub> and BaO<sub>2</sub> are similar (for BaO<sub>2</sub>,  $a = 3.811$  Å,  $c = 6.823$  Å; for KO<sub>2</sub>,  $a' = 4.033$  Å,  $c' = 6.907$  Å). Both materials can be regarded in terms of the ordered stacking of neutral atomic planes along the [001] direction, so a coherent interface without polar discontinuity can be expected in this direction. Second, the ionic radii of the K<sup>+</sup> and Ba<sup>2+</sup> cations are very similar (1.38 vs. 1.35 Å), which greatly reduces the lattice distortion in the (001) interface region. Consequently, along the [001] direction, the stacking of O<sub>2</sub>-M<sub>6</sub> (M = K/Ba) octahedra across the KO<sub>2</sub>/BaO<sub>2</sub> (001) interface should be maintained as in the two constituent bulk materials, enhancing the stability of the interface.

We first study the electronic structure and magnetic properties of the heterostructure with a sharp interface shown in Fig. 3(a) [the atomic structure of the entire heterostructure is shown in Fig. 2(a)]. The total density of states (TDOS) [shown in Fig. 4(a)] for this case shows a semiconducting gap of about 0.7 eV, which is due to the limited degree of double exchange between the O<sub>2</sub><sup>2-</sup> and O<sub>2</sub><sup>-</sup> anions. The magnetic moment per dimer, averaged over each atomic layer of this heterostructure, is shown in Table I. On the KO<sub>2</sub> side, the magnetic moments in adjacent K-O layers along the  $c$  direction follow a pattern consistent with the A-type antiferromagnetism in bulk KO<sub>2</sub> [49], and the distribution of magnetic moments in each layer is the same as that in bulk KO<sub>2</sub>. On the BaO<sub>2</sub> side, the moments are zero for every layer as expected for nonmagnetic peroxide anions.

The realization of metallicity and ferromagnetism at the KO<sub>2</sub>/BaO<sub>2</sub> (001) interface requires stronger double exchange between O<sub>2</sub><sup>2-</sup> and O<sub>2</sub><sup>-</sup> anions, which in turn is likely to require a stronger degree of mixed valency. Interface roughening can be a useful route to achieve this. Considering the similarities in



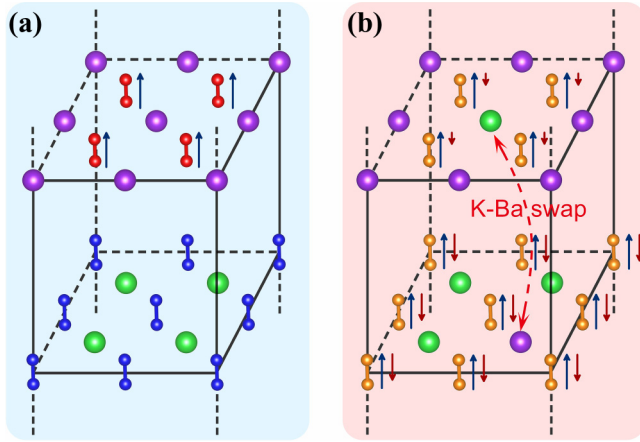


FIG. 3. Atomic structures and unpaired (or partially paired) spin(s) of each dimer for (a) the case with a sharp interface and (b) the case with a rough interface. The blue and red arrows indicate spin-up and spin-down, respectively (the paired spins associated with each dimer are not shown here). The purple and green spheres indicate K and Ba atoms, respectively. For the sharp interface, the red and blue dimers represent  $\text{O}_2^-$  and  $\text{O}_2^{2-}$ , respectively. The yellow dimers represent dioxygen anions with mixed valency for the rough interface.

ionic radius and electronegativity of K and Ba, it is reasonable to expect that the two cations are swapped on some lattice sites close to the interface, by analogy with the interfacial La-Sr interdiffusion that occurs at the widely studied  $\text{LaAlO}_3/\text{SrTiO}_3$  interface and which serves as one explanation for the 2DEG properties of this system [50].

To model such a heterostructure with a rough interface [the detailed atomic structure of this rough interface is shown in Fig. 3(b)], we use a supercell based on that with the sharp interface, but with the main difference that one  $\text{K}^+$  cation

TABLE I. Local magnetic moment per dimer averaged over each atomic layer of heterostructures with sharp and rough (swapped K-Ba) interfaces, in units of  $\mu_B$ .

| Sequence of the atomic layers | Interface with defect free | Interface with K-Ba swap |
|-------------------------------|----------------------------|--------------------------|
| K-O 6th                       | -0.83                      | -0.83                    |
| K-O 5th                       | 0.83                       | 0.83                     |
| K-O 4th                       | -0.83                      | -0.83                    |
| K-O 3rd                       | 0.83                       | 0.83                     |
| K-O 2nd                       | -0.83                      | -0.83                    |
| K-O 1st                       | 0.83                       | 0.73                     |
| Ba-O 1st                      | 0.00                       | 0.14                     |
| Ba-O 2nd                      | 0.00                       | 0.00                     |
| Ba-O 3rd                      | 0.00                       | 0.00                     |
| Ba-O 4th                      | 0.00                       | 0.00                     |
| Ba-O 5th                      | 0.00                       | 0.00                     |
| Ba-O 6th                      | 0.00                       | 0.00                     |
| Ba-O 7th                      | 0.00                       | 0.00                     |

was exchanged with one  $\text{Ba}^{2+}$  cation at the interface [the detailed atomic structure of this heterostructure is shown in Fig. 2(b)]. That is, at the interface where the first K-O layer meets the first Ba-O layer, one K in the first K-O layer is swapped with one Ba in the first Ba-O layer. This K-Ba swap can be considered as a defect complex composed of isolated  $\text{K}_{\text{Ba}}$  and  $\text{Ba}_{\text{K}}$  antisite defects at the interface. The binding energy of this defect complex [51] is calculated to be 0.12 eV, indicating that the K-Ba swap is favorable at the interface at room temperature with respect to the two isolated antisite defects.

We find that the average bond length of the dimers in the first K-O (Ba-O) layer is longer (shorter) than that of an isolated superoxide (peroxide) anion, 1.39 (1.49) versus 1.36 (1.52) Å. Therefore, the K-Ba swap renders the dimers in the interfacial layers more mixed valent compared to the case of sharp interface. The TDOS of the heterostructure with the rough interface (swapped K-Ba) is shown in Fig. 4(b), and it shows that this heterostructure is half-metallic: the spin-down channel is metallic whereas the spin-up channel exhibits a gap of about 0.2 eV. This half-metallicity can be well explained by double exchange between  $\text{O}_2^{2-}$  and  $\text{O}_2^-$  anions at the interface. Compared to the case of the sharp interface, the four dimers in the first K-O layer of our model can be considered to be doped by one electron. Before electron doping, the unpaired electron in the  $\pi^*$  orbitals of each superoxide anion in the first K-O layer has the same spin (spin up) due to the A-type antiferromagnetic order in  $\text{KO}_2$ . According to Hund's rules, the spin of the doped electron must be opposite to that of the unpaired electron, thus electrons hopping between dimers in the electron-doped first K-O layer must have the same spin (spin-down). Similarly, the four dimers in the first Ba-O layer can be considered to be doped by one hole. Before hole doping, electrons in the  $\pi^*$  orbitals of the peroxide anions in the first Ba-O layer are paired with antiparallel spins. After hole doping (loosing of one spin-down electron), the electrons hopping between dimers in the hole-doped Ba-O layer must also have the same spin direction (spin-down).

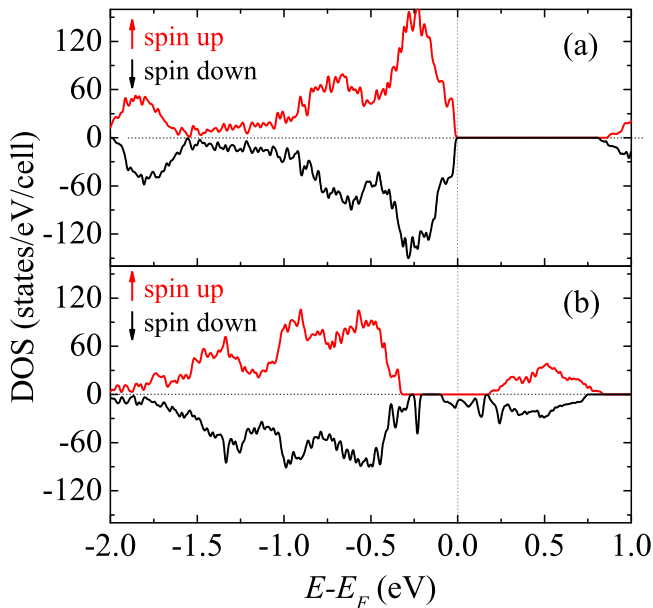


FIG. 4. Total density of states (TDOS) for (a) heterostructure with a sharp interface, (b) heterostructure with a rough interface (swapped K-Ba).

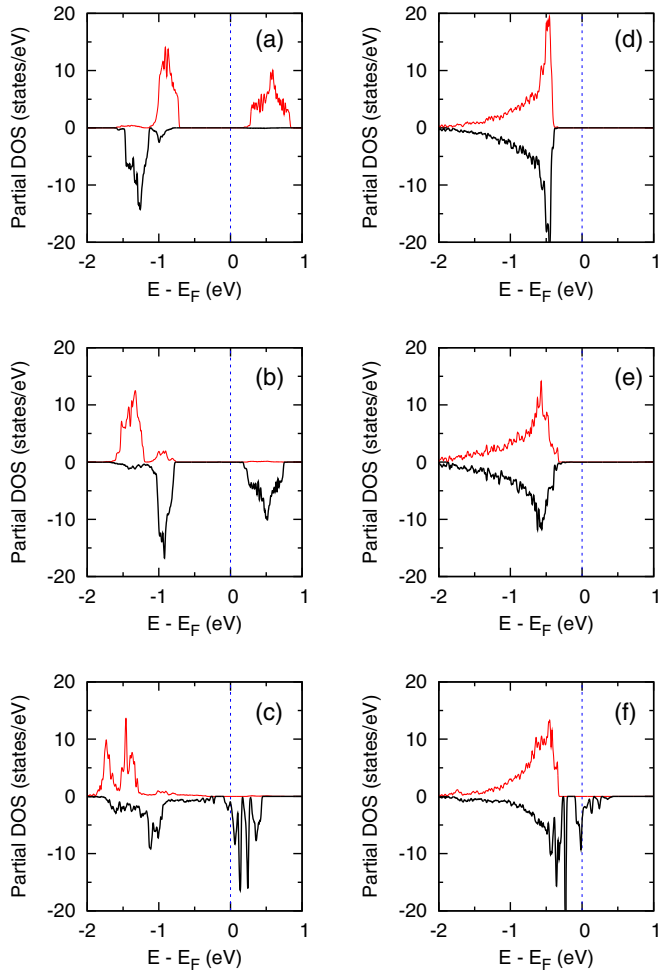


FIG. 5. Partial density of states (red and black lines indicate spin-up and spin-down) of the antibonding  $\pi^*$  orbital near the Fermi energy: (a), (b), and (c) are for dimers in the surface (sixth K-O layer), middle (third K-O layer), and interface (first K-O layer) regions of  $\text{KO}_2$  side, respectively; (d), (e), and (f) are for dimers in the surface (seventh Ba-O layer), middle (fourth Ba-O layer), and interface (first Ba-O layer) regions of  $\text{BaO}_2$  side, respectively.

Moreover, as shown in Fig. 5, we studied the partial density of states (PDOS) for dioxygen anions in the surface, middle, and interface regions of  $\text{KO}_2$  and  $\text{BaO}_2$ . Figures 5(a), 5(b) and 5(c) are for dimers in the surface, middle, and interface regions of the  $\text{KO}_2$  side, respectively; Figs. 5(d), 5(e) and 5(f) are for dimers in the surface, middle, and interface regions of  $\text{BaO}_2$  side, respectively. The PDOS for dimers in the surface and middle regions of  $\text{KO}_2$  and  $\text{BaO}_2$  sides show semiconducting character, and thus do not contribute to the density of states at the Fermi energy. The PDOS for dimers in the interfacial K-O and Ba-O layers are only nonzero at the Fermi energy for the spin-down channel. Therefore, the half-metallic conduction of the heterostructure with a rough interface is attributed only to oxygen dimers in the first K-O and first Ba-O layers, which confirms the conclusion obtained from the electron-doping and hole-doping models discussed above.

We next study the magnetic properties of the case with a rough interface. The magnetic moment per dimer, averaged over each layer of the structural model, is shown in Table I.

The magnetic moments in the first K-O layer and first Ba-O layer are all aligned in a ferromagnetic manner [52], which originates from the double exchange in the electron-doped K-O layer and hole-doped Ba-O layer. On the  $\text{KO}_2$  side of the interface, the magnetic moments are again aligned in A-type antiferromagnetic fashion with the same magnitude as for the sharp interface ( $0.83 \mu_B$ ) from the second to sixth K-O layer, while the magnetic moment per dimer in the first K-O layer is about  $0.1 \mu_B$  smaller. After one spin-down electron is transferred to the first K-O layer, the magnetic moment per dimer in this layer should be decreased by  $0.25 \mu_B$  compared to the sharp interface case. The smaller decrease that we obtain is attributed to the joint effects of the theory used in VASP to calculate the local magnetic moment of an ion and the electron itinerancy in the half-metallic interfacial K-O layer [53]. On the  $\text{BaO}_2$  side, the local magnetic moments are zero from the second to seventh Ba-O layers, while a magnetic moment of  $0.14 \mu_B$  per dimer is obtained in the first Ba-O layer instead of zero for the case with a sharp interface. The loss of one spin-down electron from the first Ba-O layer should yield a magnetic moment of  $0.25 \mu_B$  per dimer. The difference between the calculated and expected moments in the first Ba-O layer is due to the same factor as described above for the first K-O layer.

Furthermore, if the thickness of K-O atomic layers can be controlled precisely during experimental fabrication, such as an even number of K-O layers, the net magnetization of the heterostructure with a rough interface is  $0 \mu_B$  according to our calculations. The half-metallicity with zero net magnetization here can have potential application in device design of spintronics, which is similar to the advantage of a half-metallic antiferromagnets [54].

The electronic and magnetic properties of  $\text{KO}_2/\text{BaO}_2$  (001) heterostructures with sharp interfaces were also studied using different values of the Hubbard  $U$  (4 and 5 eV) and by varying the thickness of the K-O and Ba-O atomic layers (5 vs. 5, 6 vs. 6, and 6 vs. 7 layers), the semiconducting properties remain the same in all these six cases; Similar calculations were performed to heterostructures with rough interfaces, the half-metallic and ferromagnetic properties remain the same in all these six cases, which implies that the half-metallicity and ferromagnetism at interfaces with swapped K-Ba is robust.

At rough interfaces where  $\text{K}_{Ba}$  and  $\text{Ba}_K$  defect complexes are introduced, the concentration of these defects will determine the doping level of the first K-O and first Ba-O layers and should thus influence the occurrence of half-metallicity and ferromagnetism. We studied four cases with defect concentrations of 6.25% (case *a*), 12.5% (case *b*), 25% (case *c*), and 50% (case *d*) at the interface, where the shortest distances between neighboring defects are  $4a$ ,  $2\sqrt{2}a$ ,  $2a$ , and  $\sqrt{2}a$ , respectively. Figure 6 shows the TDOS for cases *a*, *b*, *c*, and *d*, respectively. From these four total density of states, we find that a minimal concentration of cation intermixing (between 12.5% and 25%) is necessary for the occurrence of half-metallicity and anionogenic ferromagnetism at the  $\text{KO}_2/\text{BaO}_2$  (001) interface. Cases *a* and *b* are both semiconducting, because of the weak double exchange in the electron-doped K-O layer (first K-O layer) and the hole-doped Ba-O layer (first Ba-O layer). Judged from the bond length of an oxygen dimer and its local magnetic moment, the doped electron in the first K-O layer is localized on one

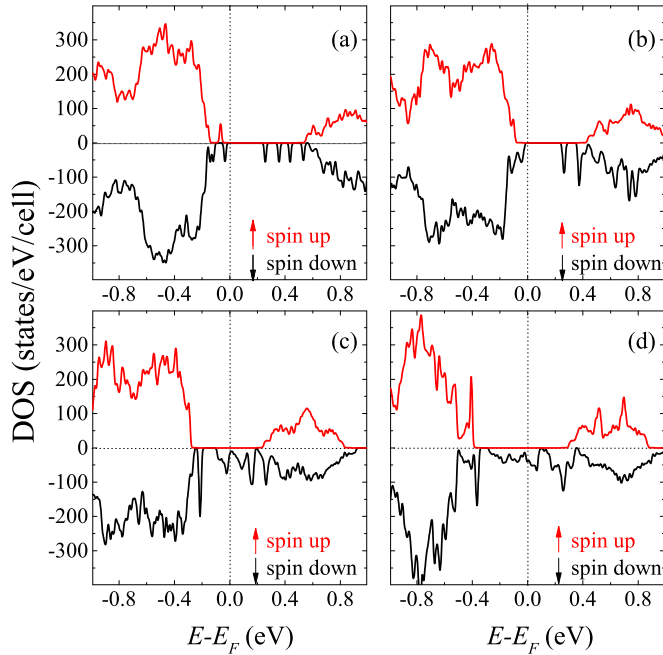


FIG. 6. Total density of states (TDOS) for cases with  $K_{Ba}/Ba_K$  defect concentration of (a) 6.25%, (b) 12.5%, (c) 25%, and (d) 50%. The red and black lines indicate spin-up and spin-down, respectively. The TDOS shown in cases (a) and (b) were obtained using supercells with 480 atoms, while the TDOS in (c) and (d) were both obtained by multiplying the real TDOS of the system (from supercells with 120 atoms) by a factor of 4 for easy comparison to the other two cases.

dimer in the form of a peroxide anion, and the other dimers remain in the form of superoxide anions in this layer. Similarly, the doped hole in the first Ba-O layer is also localized on one dimer, in the form of a superoxide anion, and the others remain in the form of peroxide anions in this layer. Cases *c* and *d* are half-metallic, because of the stronger double exchange in the electron-doped K-O layer (first K-O layer) and the hole-doped Ba-O layer (first Ba-O layer). Due to the itinerancy of electrons in the electron-doped K-O layer and hole-doped Ba-O layer, the oxygen dimers in the first K-O layer are equivalent, and the ones in the first Ba-O layer are also equivalent. Comparing these four cases with each other, we find that an increase in the concentration of  $K_{Ba}$  and  $Ba_K$  defect complexes decreases the shortest distance between neighboring defects and strengthens the double exchange between oxygen dimers, leading to a transition from semiconductor to half-metal.

It is possible that disorder of dopants in the interfacial region can exist, and it competes with double exchange, which may suppress the half-metallicity and ferromagnetism. We also note that the stability of half-metallicity and ferromagnetism at the  $2p$ -insulator heterointerfaces can be more complex because some other factors may exist, such as the electron-phonon coupling. Consequently, for a detailed study on the stability of half-metallicity and ferromagnetism at the interface we leave this to future experiments and theoretical studies. It is worth mentioning that here we discuss different degrees of cation intermixing at the interface, all discussions in the rest of the parts of this paper correspond to the case where the degree of cation intermixing is 25%.

In the field of  $2p$  magnetism, most of the published theoretical work [6,9,13] choose the technique DFT +  $U$  to treat the correlation effects in this class of correlated materials. Specifically, based on this technique, theoretical predictions [13] on the thermal libration of superoxide anions and the formation of orbital ordering in correlated  $2p$  insulator  $CsO_2$  were confirmed by later experimental findings [15,23]. Moreover, in strongly correlated transition metal oxides, the technique DFT + DMFT is widely used. In cases where the electron correlation is not very strong, the technique DFT +  $U$  can be used, and it can be regarded as the static limit of the technique DFT + DMFT. The electron correlation in correlated  $2p$  materials is expected to be weaker than that in strongly correlated  $3d$  materials (such as the electron or hole-doped Mott insulators), consequently the technique DFT +  $U$  should be valid for correlated  $2p$  insulators. For the  $2p$ -insulator heterointerfaces with electron or hole-doping, we perform calculations based on the technique DFT +  $U$ , and a ferromagnetic and half-metallic interface is found. Theoretical studies on doped  $2p$  Mott insulators using techniques DFT + DMFT and DFT +  $U$ , and a systematic comparison of conclusions obtained from these two techniques as well, are desired for future work. Specifically, experiments testing the validity of both DFT +  $U$  and DFT + DMFT techniques used to deal with the correlation effect in the field of  $2p$  magnetism are desired in the future.

#### IV. SUMMARIES AND CONCLUSION

Compared to the mixed-valent sesquioxides with insulating spin-glass character [18], the rough  $KO_2/BaO_2$  (001) interface has several advantages. First, the strength of double exchange at the interface can be tuned by the concentration of defects, which might be controllable during interface fabrication. Second, the electronic and magnetic properties of the interface can likely be tuned by strain engineering. Third, the half-metallicity and long-range ferromagnetism are quasi-two-dimensional, confined to the interface region. Finally, under precise control over the thickness of K-O atomic layers, the half-metallicity with zero net magnetization can be realized.

In conclusion, we use first-principles calculations to predict half-metallicity and long-range anionogenic ferromagnetism at the (001) heterointerface between two  $2p$  insulators  $KO_2$  and  $BaO_2$ . When  $K^+$  and  $Ba^{2+}$  cations with a minimal concentration in the interfacial layers are swapped, these layers become electron-doped or hole-doped, enhancing the degree of double exchange and promoting the half-metallic and ferromagnetic state. The prediction of half-metallicity and long-range ferromagnetism and their mechanisms reported here can serve as a useful guide to the experimental fabrication of such heterostructures. These systems consist of  $2p$  insulators, and could constitute a new family of heterostructures of both scientific and technological importance, even with enhanced properties compared to currently widely studied heterostructures based on  $3d$  insulators.

#### ACKNOWLEDGMENTS

We thank G. A. de Wijs and M. Zhao for their useful discussions, and also appreciate three anonymous

referees for their valuable suggestions and comments. This work is supported by the Natural Science Foundation of

Shandong Province (CN) with Grants No. ZR2016AB12 and ZR2015AL020.

- [1] J. J. Attema, G. A. de Wijs, G. R. Blake, and R. A. de Groot, *J. Am. Chem. Soc.* **127**, 16325 (2005).
- [2] R. J. Meier and R. B. Helmholtz, *Phys. Rev. B* **29**, 1387 (1984).
- [3] M. Kim and B. I. Min, *Phys. Rev. B* **84**, 073106 (2011).
- [4] W. Hesse, M. Jansen, and W. Schnick, *Prog. Solid State Chem.* **19**, 47 (1989).
- [5] J. Winterlik, G. H. Fecher, C. Felser, C. Mühle, and M. Jansen, *J. Am. Chem. Soc.* **129**, 6990 (2007).
- [6] J. Winterlik, G. H. Fecher, C. A. Jenkins, C. Felser, C. Mühle, K. Doll, M. Jansen, L. M. Sandratskii, and J. Kübler, *Phys. Rev. Lett.* **102**, 016401 (2009).
- [7] M. Kim, B. H. Kim, H. C. Choi, and B. I. Min, *Phys. Rev. B* **81**, 100409(R) (2010).
- [8] R. Kováčik and C. Ederer, *Phys. Rev. B* **80**, 140411(R) (2009).
- [9] A. K. Nandy, P. Mahadevan, P. Sen, and D. D. Sarma, *Phys. Rev. Lett.* **105**, 056403 (2010).
- [10] E. R. Ylvisaker, R. R. P. Singh, and W. E. Pickett, *Phys. Rev. B* **81**, 180405(R) (2010).
- [11] K. Wohlfeld, M. Daghofer, and A. M. Olés, *Europhys. Lett.* **96**, 27001 (2011).
- [12] M. Kim and B. I. Min, *Phys. Rev. B* **89**, 121106(R) (2014).
- [13] S. Riyadi, B. Zhang, R. A. de Groot, A. Caretta, P. H. M. van Loosdrecht, T. T. M. Palstra, and G. R. Blake, *Phys. Rev. Lett.* **108**, 217206 (2012).
- [14] I. V. Solovyev, Z. V. Pchelkina, and V. V. Mazurenko, *Cryst. Eng. Comm.* **16**, 522 (2014).
- [15] T. Knaflič, M. Klanjšek, A. Sans, P. Adler, M. Jansen, C. Felser, and D. Arčon, *Phys. Rev. B* **91**, 174419 (2015).
- [16] S. Riyadi, S. Giriya-pura, R. A. de Groot, A. Caretta, P. H. M. van Loosdrecht, T. T. M. Palstra, and G. R. Blake, *Chem. Mater.* **23**, 1578 (2011).
- [17] J. Winterlik, G. H. Fecher, C. A. Jenkins, S. Medvedev, C. Felser, J. Kübler, C. Mühle, K. Doll, M. Jansen, T. Palasyuk, I. Trojan, M. I. Eremets, and F. Emmerling, *Phys. Rev. B* **79**, 214410 (2009).
- [18] S. Giriya-pura, B. Zhang, R. A. de Groot, G. A. de Wijs, A. Caretta, P. H. M. van Loosdrecht, W. Kockelmann, T. T. M. Palstra, and G. R. Blake, *Inorg. Chem.* **53**, 496 (2014).
- [19] S. Giriya-pura, Ph.D. Thesis, University of Groningen, The Netherlands, 2012.
- [20] R. Kováčik, P. Werner, K. Dymkowski, and C. Ederer, *Phys. Rev. B* **86**, 075130 (2012).
- [21] D. Arčon, K. Anderle, M. Klanjšek, A. Sans, C. Mühle, P. Adler, W. Schnelle, M. Jansen, and C. Felser, *Phys. Rev. B* **88**, 224409 (2013).
- [22] A. Sans, J. Nuss, G. H. Fecher, C. Mühle, C. Felser, and M. Jansen, *Z. Anorg. Allg. Chem.* **640**, 1239 (2014).
- [23] M. Klanjšek, D. Arčon, A. Sans, P. Adler, M. Jansen, and C. Felser, *Phys. Rev. Lett.* **115**, 057205 (2015).
- [24] I. V. Solovyev, *New J. Phys.* **10**, 013035 (2008).
- [25] S. Naghavi, S. Chadov, C. Felser, G.H. Fecher, J. Kübler, K. Doll, and M. Jansen, *Phys. Rev. B* **85**, 205125 (2012).
- [26] C. Zener, *Phys. Rev.* **82**, 403 (1951).
- [27] P. W. Anderson and H. Hasegawa, *Phys. Rev.* **100**, 675 (1955).
- [28] E. Dagotto, T. Hotta, and A. Moreo, *Phys. Rep.* **344**, 1 (2001).
- [29] A. Ohtomo and H. Y. Hwang, *Nature (London)* **427**, 423 (2004).
- [30] R. Pentcheva and W. E. Pickett, *Phys. Rev. Lett.* **99**, 016802 (2007).
- [31] N. Reyren, S. Thiel, A. D. Caviglia, L. F. Kourkoutis, G. Hammerl, C. Richter, C. W. Schneider, T. Kopp, A.-S. Rüetschi, D. Jaccard, M. Gabay, D. A. Muller, J.-M. Triscone, and J. Mannhart, *Science* **317**, 1196 (2007).
- [32] A. Brinkman, M. Huijben, M. Van Zalk, J. Huijben, U. Zeitler, J. C. Maan, W. G. Van der Wiel, G. Rijnders, D. H. A. Blank, and H. Hilgenkamp, *Nat. Mater.* **6**, 493 (2007).
- [33] L. Li, C. Richter, J. Mannhart, and R. C. Ashoori, *Nat. Phys.* **7**, 762 (2011).
- [34] B. Kalisky, J. A. Bert, B. B. Klopfer, C. Bell, H. K. Sato, M. Hosoda, Y. Hikita, H. Y. Hwang, and K. A. Moler, *Nat. Commun.* **3**, 922 (2012).
- [35] J. A. Bert, B. Kalisky, C. Bell, M. Kim, Y. Hikita, H. Y. Hwang, and K. A. Moler, *Nat. Phys.* **7**, 767 (2011).
- [36] K. S. Takahashi, M. Kawasaki, and Y. Tokura, *Appl. Phys. Lett.* **79**, 1324 (2001).
- [37] B. R. K. Nanda, S. Satpathy, and M. S. Springborg, *Phys. Rev. Lett.* **98**, 216804 (2007).
- [38] C. He, A. J. Grutter, M. Gu, N. D. Browning, Y. Takamura, B. J. Kirby, J. A. Borchers, J. W. Kim, M. R. Fitzsimmons, X. Zhai, V. V. Mehta, F. J. Wong, and Y. Suzuki, *Phys. Rev. Lett.* **109**, 197202 (2012).
- [39] J. P. Perdew, K. Burke, and M. Ernzerhof, *Phys. Rev. Lett.* **77**, 3865 (1996).
- [40] P. E. Blöchl, *Phys. Rev. B* **50**, 17953 (1994).
- [41] G. Kresse and D. Joubert, *Phys. Rev. B* **59**, 1758 (1999).
- [42] G. Kresse and J. Furthmüller, *Phys. Rev. B* **54**, 11169 (1996).
- [43] G. Kresse and J. Furthmüller, *Comput. Mater. Sci.* **6**, 15 (1996).
- [44] G. Kresse and J. Hafner, *Phys. Rev. B* **49**, 14251 (1994).
- [45] G. Kresse and J. Hafner, *Phys. Rev. B* **47**, 558(R) (1993).
- [46] S. L. Dudarev, G. A. Botton, S. Y. Savrasov, C. J. Humphreys, and A. P. Sutton, *Phys. Rev. B* **57**, 1505 (1998).
- [47] M. Ziegler, M. Rosenfeld, W. Känzig, and P. Fischer, *Helv. Phys. Acta* **49**, 57 (1976).
- [48] W. Wong-Ng and R. S. Roth, *Physica C (Amsterdam)* **233**, 97 (1994).
- [49] H. G. Smith, R. M. Nicklow, L. J. Raubenheimer, and M. K. Wilkinson, *J. Appl. Phys.* **37**, 1047 (1966).
- [50] P. R. Willmott, S. A. Pauli, R. Herger, C. M. Schlepütz, D. Martoccia, B. D. Patterson, B. Delley, R. Clarke, D. Kumah, C. Cionca, and Y. Yacoby, *Phys. Rev. Lett.* **99**, 155502 (2007).
- [51] C. Freysoldt, B. Grabowski, T. Kichel, J. Neugebauer, G. Kresse, A. Janotti, and G. C. Vandewal, *Rev. Mod. Phys.* **86**, 253 (2014).
- [52] The magnetic moments in the first K-O layer are all in parallel with those in the first Ba-O layer. The robustness of this result was further checked by DFT calculations with various antiferromagnetic spin configurations (both interlayer and intralayer antiferromagnetic spin configurations). All models converged to the same ferromagnetic state.

- [53] On one hand, VASP only summarizes the magnetization in a sphere with Wigner Seitz radius and omits the contribution of any interstitial magnetization when calculating the local magnetic moment of an ion. On the other hand, the electron itineracy at the half-metallic interface here could render the difference between the calculated and expected magnetization even larger compared to that in semiconducting or insulating cases with strong electron localization.
- [54] H. van Leuken and R. A. de Groot, [Phys. Rev. Lett. \*\*74\*\*, 1171 \(1995\)](#).